

Depth-multiplexing spectral domain OCT for full eye length imaging with a single modulation unit

GUANGHAN MENG^{*†}, ANDREW ZHANG^{*}, FABIO FEROLDI, AUSTIN ROORDA, AND LAURA WALLER[†]

University of California Berkeley, Berkeley, California, USA, 94720

**The authors contributed equally to this research.*

†guanghan_meng@berkeley.edu; waller@berkeley.edu

Abstract: Measuring the axial length of the eye is emerging as a crucial approach to measure progression and monitor management of myopia. The high cost of current swept-source OCT devices, the preferred method for such measurements, limits their broad use, especially in lower-income communities. While spectral domain (SD) OCT is a more affordable option, its limited imaging range falls short for full eye length measurement. Existing depth-multiplexing (DM) techniques for SD-OCT provide a workaround by capturing images at multiple depths within the eye. However, these methods typically require multiple light modulation units or detectors for simultaneous imaging across depths, adding complexity and cost. In response, we propose a novel DM-SD-OCT approach that utilizes a single light modulation unit for depth encoding. This innovative method facilitates the capture of images at multiple depths within the eye using a single line scan camera, with subsequent computational demixing. Our implementation of this system successfully enabled simultaneous acquisition and demixing of signals from three distinct depths within the eye. The system's effectiveness was demonstrated using a model eye, confirming its potential as a cost-effective solution for comprehensive eye length measurement in clinical myopia research.

Myopia stands as a pervasive global issue that is progressively worsening [1]. Despite its widespread prevalence, a definitive cure remains elusive. Axial eye length measurement offers heightened sensitivity to track the eye's elongation, a characteristic of myopia progression, and holds the potential to detect changes within the eye even before pediatric patients begin to exhibit visual consequences. Swept-source OCT devices are the gold standard for axial eye length measurement in clinics, but the costs limit its availability to resource-rich clinics only. Introducing an affordable OCT device for axial eye length measurement, accessible across a spectrum of eye clinics including community healthcare centers, has the potential to reshape routine eye examinations. This becomes all the more pivotal considering the global prevalence of myopia.

Recently, thermally tuned vertical cavity surface emitting lasers (VCSEL) have been employed for low-cost full-eye swept-source OCT [2, 3], but the low-cost VCSEL originally designed for lidar is limited in optical output power and tuning bandwidth. Spectral domain (SD) OCT is more cost-effective than SS-OCT, but it faces the limitation of confined imaging range beyond the reference mirror depth. The integration of multiple reference arms targeting different depths within the eye has been explored to overcome this constraint of SD-OCT, and related approaches fall into two categories: sequential acquisition and simultaneous acquisition. Sequential acquisition alternates between different arms for data collection [4–8], thus sacrificing temporal resolution. In contrast, simultaneous acquisition methods generally integrate multiple interferometers or optical modulation devices, one for each reference arm [9–14]. As a result, these methods amplify costs and bulkiness, thus compromising accessibility and portability. Although a single-interferometer-based depth-multiplexing strategy has been developed for SS-OCT [15–17], it relies on coherence revival of the SS-laser and is not applicable to SD-OCT. Furthermore, the method lies with the polarization division of light in the sample arm, introducing additional loss

of the signal reflected from the eye and demanding more power to be delivered to the subject's eye.

Here, we propose a novel depth-multiplexing technique that aims to address all the above issues and holds broad applicability across all spectral domain OCT systems seeking enhanced imaging depth in ophthalmology applications. The single-interferometer-based technique employs a solitary scanning mirror to encode distinct phase ramps for multiple reference arms, facilitating simultaneous data acquisition of the entire eye length with a single scan. Furthermore, as the light division happens in the reference arm and is polarization independent, reflected signal from the sample arm does not experience light loss on its way back, in contrast to the existing polarization-dependent depth-multiplexing strategy. Additionally, although previous depth-multiplexing strategies generally involve two reference arms only, our power-efficient and single-modulation unit-based method enables simultaneous capturing and computational demixing of signal from three different depths.

Previously, a phase-shift method achieved by deviating the light beam from the pivot axis of the galvanometer scanner [18–20] was developed to remove the complex conjugate artifact in OCT image reconstruction. The off-center distance of the incident beam from the pivot axis induces an optical path length (OPL) change as the galvanometer scans around its rotation axis, resulting in a linear phase ramp along the slow axis of the B-scan image. By applying a Hilbert transform (HT) to the Fourier-domain signal along the lateral-scanning direction (the slower axis in a B-scan), both amplitude and phase components can be recovered, which are sufficient to suppress the complex conjugate artifact in the reconstruction.

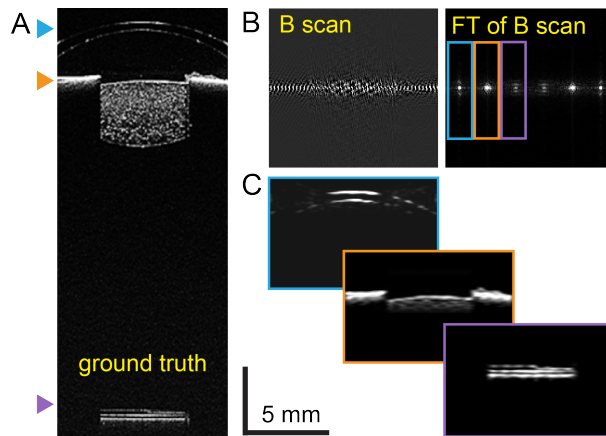


Fig. 1. Principle of frequency-encoded depth multiplexing demonstrated by simulation. (A) Model eye image input into the simulation pipeline. Arrowheads: the depths of three reference arms. (B) Simulated frequency-encoded B scan. Left: simulated cross-correlation term in the B scan. Right: Fourier transform of the B scan along the transverse axis. Boxes: the spectrum peaks corresponding to the three depths in (A). (C) Reconstructed images from the three cropped spectra in (B)

Our depth-multiplexing (DM) SD-OCT method is an extension of this phase-modulation approach. Three reference arms targeting the front, middle, and back of the eye, are simultaneously modulated by a separate galvanometer introduced to the reference arm set (called reference scanner from now) and imaged with the same interferometer (Fig. 1). The reference scanner is synchronized with the fast scanner in the sample arm, and reference beams with varying OPLs are directed onto the reference scanner at different positions, resulting in distinct phase ramps along the transverse axis of the B scan. The phase ramps allow signal from different depths to be demixed via a Fourier transform of the B scan along the transverse axis [9] (Fig. 1B,C).

The modulated OPL of the reference arm can be given by $\Delta z_r = 2s \tan(\theta)$, where θ is the angle between the incident beam and the galvo normal direction, s is the off-center distance of the incident beam. When the reference scanner is centered around $\theta = 45^\circ$, we get $\Delta z_r \approx 2s(1 + 2(\theta - \pi/4)) \approx 4s\Delta\theta = 4s\omega/r$, where ω is the angular speed of the galvo, and r the line scan rate of the system. Therefore, the slope of the phase ramp between each pair of adjacent line scans is

$$\phi = k\Delta z_r = 4ks\frac{\omega}{r}, \quad (1)$$

where k is the central wavenumber. The specific phase shifts for the multiple reference arms should be selected based on the spectrum width and shape of the spectrum after the HT. If the spectra are expected to be clean and uniform, and the n reference arms each occupy $1/n$ of the full π phase range in the quadrant, then the phase shift for the i th reference arm (1st arm is closest to the rotation axis) is:

$$\phi_i = \frac{(2i-1)\pi}{2n}. \quad (2)$$

Based on equations 1 and 2, the off-center distance for the i th reference arm is:

$$s_i = \frac{\phi_i}{4k} \frac{r}{\omega} = \frac{(2i-1)\pi}{8kn} \frac{r}{\omega} = \frac{(2i-1)\lambda}{16n} \frac{r}{\omega}. \quad (3)$$

Therefore, when there are 3 reference arms, we will have:

$$s_i = \frac{(2i-1)\lambda}{48} \frac{r}{\omega}. \quad (4)$$

We used a low-cost line camera (Spyder3 1k, Teledene Dalsa) along with a holographic grating (HD 1800, Wasatch Photonics) to build a spectrometer, and off-the-shelf optics from Thorlabs Inc. for all other parts in our system. The key components in the reference arm set includes two cube beam splitters (BS005 and BS053), a 5x beam reducer (GBE05-B), a scanner (GVS011), and a lenslet array (MLA12) (Fig. 2). The lenslet array is critical to reflect light with different OPLs back to the correct path, and has a pitch of 1.0mm by 1.4mm. We used the 1.0mm separation distance between beams on the reference scanner to match the 1.0mm pitch, i.e., the off-center distances for the three beams are $s_1 = 0.5$ mm (retina arm), $s_2 = 1.5$ mm (lens arm), and $s_3 = 2.5$ mm (cornea arm). Given the 830nm central wavelength for our light source (SLD830S-A20W, 55 nm bandwidth, Thorlabs Inc.), the optimal step size of our galvo is determined as $\omega/r = 34.58 \mu\text{rad}/\text{line}$. We thus chose to use a mechanical scanning angle of $\pm 0.8^\circ = \pm 0.01396$ rad, which gives an actual step size of $\omega/r = 35.80 \mu\text{rad}$. This results in an expected phase ramp of 0.542 rad/line, 1.63 rad/line, and 2.71 rad/line for arms 1, 2, and 3, respectively. These phase ramps shift the spectra centers of the three reference arms to $\pi/6$, $\pi/2$, and $5\pi/6$, respectively.

Signal fall-off and reference arm depths characterization were performed using a protected silver mirror as the sample. The home-built spectrometer using off-the-shelf optics and a low-cost line scan camera gives a 0.11 nm spectral resolution, resulting in a 1.4 mm imaging range within 6dB signal fall-off (Fig. 3). The depths of the three reference arms are centered around 0 μm , 4531 μm , and 36512 μm , respectively (Fig. 3). With a 3 μs camera exposure time (corresponding to a 300 kHz A-scan rate), we achieved a peak signal-to-noise (SNR) above 90 dB at all three depths (Fig. 3). The axial resolution of our system is 14.4 μm .

As the proof-of-concept demonstration, we imaged a model eye (Rowe Technologies Inc.) with our DM-SD-OCT system. As in Fig. 4, using two reference arms, we successfully captured and demixed the images of the cornea and the retina (Fig. 4 A) using the frequency demixing method (Fig. 1). More specifically, by equally dividing the $0 - \pi$ phase quadrant of the B-scan's Fourier transform along the transverse axis into two segments, the retina image was reconstructed

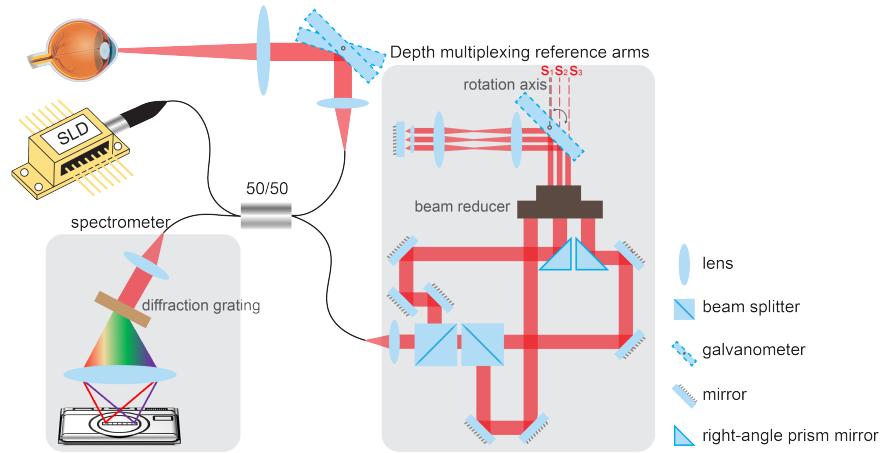


Fig. 2. Design of the DM-SD-OCT setup.

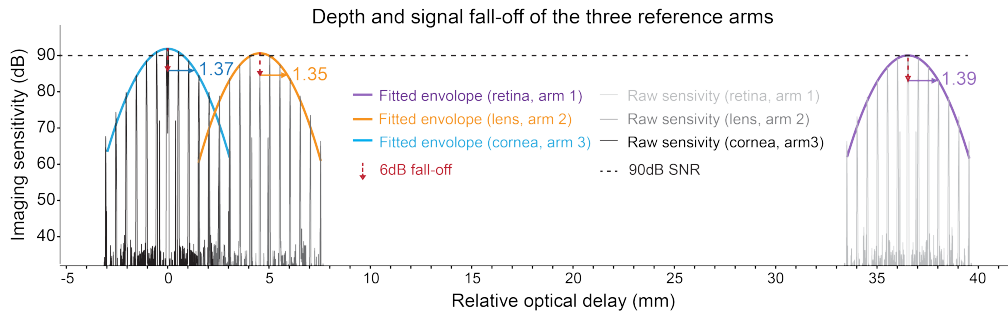


Fig. 3. Characterization of the DM-SD-OCT system.

from the $0 - \pi/2$ range while the cornea from the $\pi/2 - \pi$ range. This setting is sufficient for axial eye length measurement, but does not provide information about the anterior chamber depth (ACD). By adding an additional reference arm whose OPL matches the pupil, such information becomes available (Fig. 4B). However, due to noise introduced by galvanometer vibration, in practice, the frequency spectra from the three depths are not as isolated as in the simulation (Fig. 1), leading to cross-talk among images after frequency demixing ($0 - \pi/3$ range for the retina, $\pi/3 - 2\pi/3$ for the pupil, and $2\pi/3 - \pi$ for the cornea, respectively). To suppress the cross-talk, we minimized the correlations, i.e., dot products, among the three images obtained from the initial frequency demixing. This was achieved by reassigning the energy of each pixel across all images to the image exhibiting the highest brightness at that particular location, as determined after the initial demixing process. (Fig. 4C). Dimensions of the eye structures measured with our DM-SD-OCT match those from Zeiss IOL Master 700 (1). For example, the OPL of the axial length (AL) is measured as 35.47 mm, corresponding to a geometrical length of 25.99 mm [21], in agreement with the 26.04 mm value measured with IOL Master 700. Central corneal thickness (CCT), aqueous depth (AQD) and anterior chamber depth (ACD) also match the IOL Master readings [22].

In summary, we proposed a novel depth-multiplexing method for SD-OCT using a single phase modulation unit, without the need for additional detector. The method offers a low-cost alternative for full-eye length measurement, and is widely applicable to any SD-OCT devices where an extended imaging depth is desired. The current drawbacks include reduced dynamic range of the spectrometer when multiple arms are simultaneously captured by the same sensor,

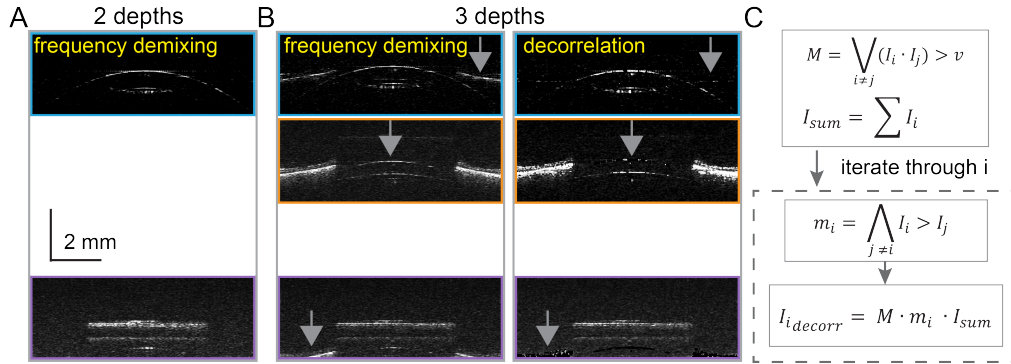


Fig. 4. Experimental validation using a model eye. (A) DM SD-OCT result after frequency demixing, with 2 reference arm depths. (B) DM SD-OCT result using 3 reference arm depths, after frequency demixing (left), and after an additional decorrelation step (right). (C) Flow chart for the decorrelation step. I_i : input images obtained with initial frequency demixing as in (B). M : the binary mask where the correlation (dot product) of any pair of images is above a user-defined value v . I_{sum} : the sum of all input images. m_i : the mask for the i^{th} decorrelated image. $I_{i_{decorr}}$: the i^{th} decorrelated output image.

	DM SD-OCT	Zeiss IOL Master
Axial length (AL)	25.99 mm	26.04 mm
Central corneal thickness (CCT)	512.0 μm	514.0 μm
Aqueous depth (AQD)	3.22 mm	3.12 mm
Anterior chamber depth(ACD)	3.73 mm	3.64 mm

Table 1. Measurement comparison between DM SD-OCT and Zeiss IOL Master 700.

although this was not a concern for our experiments. As a proof of concept demonstration, we adopted a free-space optics setup for the reference arm set, which offers high degrees of freedom in alignment and adjustable arm lengths. To make the system more compact, a fiber-based module for beam splitting and delaying can be adopted, with a miniaturized lenslet array collimator. For *in vivo* measurements, where the subjects' eye lengths vary from patient to patient, mirrors controlling the optical delay of the retina reference arm can be translated during the initial alignment process to locate the retina, which will be demonstrated in future work. Additionally, considering the well-defined shapes and sparsity of eye structures, deep learning algorithms can potentially be developed to directly demix signals from different depths, completely ruling out the need for frequency modulation and demixing.

Funding. This work was funded by the Center for Innovation in Vision and Optics, University of California, Berkeley.

Acknowledgement. G. Meng was funded by the Center for Innovation in Vision and Optics.

Disclosures. G. Meng and L. Waller filed a provisional patent: "Single modulation unit-based depth-multiplexing strategy for spectral domain optical coherence tomography (OCT)", B24-019.

Data availability. Data and code will be available upon reasonable request to correspondence authors.

References

1. B. A. Holden, T. R. Fricke, D. A. Wilson, *et al.*, “Global prevalence of myopia and high myopia and temporal trends from 2000 through 2050,” *Ophthalmology* **123**, 1036–1042 (2016).
2. S. Moon and E. S. Choi, “VCSEL-based swept source for low-cost optical coherence tomography,” *Biomed. Opt. Express* **8**, 1110–1121 (2017).
3. M. Kendrisic, V. Agafonov, M. Salas, *et al.*, “Thermally tuned VCSEL at 850 nm as a low-cost alternative source for full-eye SS-OCT,” *Opt. Lett.* **48**, 3079–3082 (2023).
4. C. Dai, C. Zhou, S. Fan, *et al.*, “Optical coherence tomography for whole eye segment imaging,” *Opt. Express* **20**, 6109–6115 (2012).
5. C. Dai, S. Fan, X. Chai, *et al.*, “Dual-channel spectral-domain optical-coherence tomography system based on 3×3 fiber coupler for extended imaging range,” *Appl. Opt.* **53**, 5375–5379 (2014).
6. M. Ruggeri, S. R. Uhlhorn, C. D. Freitas, *et al.*, “Imaging and full-length biometry of the eye during accommodation using spectral domain OCT with an optical switch,” *Biomed. Opt. Express* **3**, 1506–1520 (2012).
7. H. Wang, Y. Pan, and A. M. Rollins, “Extending the effective imaging range of Fourier-domain optical coherence tomography using a fiber optic switch,” *Opt. Lett.* **33**, 2632–2634 (2008).
8. L. Feng, L. Zhu, Q. Li, *et al.*, “Measurement of intraocular distances in human eyes by using Fourier domain low-coherence interferometry,” *Proc. SPIE* **9693** (2016).
9. S. M. R. M. Nezam, B. J. Vakoc, A. E. Desjardins, *et al.*, “Increased ranging depth in optical frequency domain imaging by frequency encoding,” *Opt. Lett.* **32**, 2768–2770 (2007).
10. C. Baker and M. J. Everett, “Optical coherence tomography for eye-length measurement,” Google Patents (2008).
11. Y. Zhou and K. O’hara, “Optical coherence tomography for eye-length measurement,” Google Patents (2009).
12. S. Fan, Y. Sun, X. Yang, *et al.*, “Whole eye segment imaging and measurement with dual-channel spectral-domain OCT,” *Ophthalmic Surgery, Lasers Imaging Retin.* **46**, 186–194 (2015).
13. T. H. Ko, Y. Zhao, and D. Huang, “Extended range imaging,” Google Patents (2013).
14. T. Wu, Q. Wang, Y. Liu, *et al.*, “Extending the effective ranging depth of spectral domain optical coherence tomography by spatial frequency domain multiplexing,” *Appl. Sci.* **6** (2016).
15. A. H. Dhalla, D. Nankivil, T. Bustamante, *et al.*, “Simultaneous swept source optical coherence tomography of the anterior segment and retina using coherence revival,” *Opt. Lett.* **37**, 1883–1885 (2012).
16. R. P. McNabb, J. Polans, B. Keller, *et al.*, “Wide-field whole eye OCT system with demonstration of quantitative retinal curvature estimation,” *Biomed. Opt. Express* **10**, 338–355 (2019).
17. A. N. Kuo, R. P. McNabb, and J. A. Izatt, “Advances in whole-eye optical coherence tomography imaging,” *The Asia-Pacific J. Ophthalmol.* **8**, 99–104 (2019).
18. B. Baumann, M. Pircher, E. Götzinger, and C. K. Hitzenberger, “Full range complex spectral domain optical coherence tomography without additional phase shifters,” *Opt. Express* **15**, 13375–13387 (2007).
19. R. A. Leitgeb, R. Michaely, T. Lasser, and S. C. Sekhar, “Complex ambiguity-free Fourier domain optical coherence tomography through transverse scanning,” *Opt. Lett.* **32**, 3453–3455 (2007).
20. R. Leitgeb, T. Lasser, A. Bachmann, *et al.*, “Optical imaging system with extended depth of focus,” Google Patents (2009).
21. T. Olsen, “Calculation of intraocular lens power: a review,” *Acta Ophthalmol. Scand.* **85**, 472–485 (2007).
22. X. Ruan, G. Yang, Z. Xia, *et al.*, “Agreement of anterior segment parameter measurements with CASIA 2 and IOLMaster 700,” *Front. Med.* **9**, 777443 (2022).